Multi-omics profiling reveals Chitinase-3-like protein 1 as a key mediator in the crosstalk between sarcopenia and liver cancer

Di Lu [a,b,e,1], Zuyuan Lin [a,b,e,1], Rui Wang [a,b,e,1], Zun Chen [a,b,e], Jianyong Zhuo [a,b,e], Li Xu [c], Linhui Pan [a,b,e], Huihui Li [a,b,e], Xinyu Yang [a,b,e], Chiyu He [a,b,e], Wei Shen [a,b,e], Modan Yang [a,b,e], Huigang Li [a,b,e], Hao Chen [a,b,e], Winyen Tan [a,e], Xuyong Wei [a,b,e], Shusen Zheng [c,d,e], Xiao Xu [a,b,c,e,*]

[a] Key Laboratory of Integrated Oncology and Intelligent Medicine of Zhejiang Province, Department of Hepatobiliary and Pancreatic Surgery, Affiliated Hangzhou First People's Hospital, Zhejiang University School of Medicine, Hangzhou, 310006, China
[b] Westlake Laboratory of Life Sciences and Biomedicine, Hangzhou, 310024, China
[c] Department of Hepatobiliary and Pancreatic Surgery, First Affiliated Hospital, Zhejiang University School of Medicine, Hangzhou, 310000, China
[d] Department of Hepatobiliary and Pancreatic Surgery, Shulan (Hangzhou) Hospital, Hangzhou, 310000, China
[e] Institute of Organ Transplantation, Zhejiang University, Hangzhou, 310003, China

ARTICLE INFO

ABSTRACT

Sarcopenia is prevalent in patients with hepatocellular carcinoma (HCC), and can adversely affect their outcomes. This study aims to explore the key mechanisms in the crosstalk between sarcopenia and HCC based on multi-omics profiling. A total of 136 male patients with HCC were enrolled. Sarcopenia was an independent risk factor for poor outcomes after liver transplantation ($p < 0.05$). Inflammatory cytokine and metabolomic profiling on these patients identified elevated plasma sTNF-R1/CHI3L1 and dysregulated lipid metabolism as related to sarcopenia and tumor recurrence risk concurrently ($p < 0.05$). Integrated analysis revealed close relationship between CHI3L1 and fatty acid metabolism. In mouse cachectic models by intraperitoneal injection of H22 cells, CHI3L1 was significantly elevated in the atrophic muscle tissue, as well as in circulation. In-vitro, CHI3L1 was up-regulated in muscle cells to protect itself from inflammatory damage through TNF-α/TNF-R1 signaling. CHI3L1 secreted by the muscle cells promoted the invasion of co-cultured HCC cells. Tumor tissue transcriptome data for 73 out of the 136 patients revealed that CHI3L1 may regulate fatty acid metabolism and oxidative stress. In vitro, CHI3L1 caused ROS and lipid accumulation. Targeted lipid profiling further proved that CHI3L1 was able to activate arachidonic acid metabolism, leading to lipid peroxide (LPO) accumulation. Meanwhile, LPO inhibition could compromise the remarkable pro-cancerous effects of CHI3L1. In conclusion, sarcopenia adversely affects the outcomes of liver transplantation for HCC. In sarcopenic patients, CHI3L1 was up-regulated and secreted by the skeletal muscle to protect itself through TNF-α/TNF-R1 signaling, which, in turn, can promote HCC tumor progression by inducing LPO accumulation.

1. Introduction

Liver cancer is the sixth most prevalent cancer and the fourth leading cause of cancer-related death in the world [1]. Among them, around 90% are hepatocellular carcinoma (HCC). It is estimated that China takes up around 55% of newly diagnosed HCC as well as 45% of HCC-related mortality [2]. Although the treatment strategies have been

significantly improved, the long-term survival still remains poor owing to its high malignancy [3]. HCC is often accompanied by liver cirrhosis, featured by malfunction in the synthesis of necessary proteins. And when diagnosed, most of the patients are already in a relatively late stage, and the tumor may have already been undermining the physiological homeostasis. Therefore, HCC patients usually have a poor nutritious status, which, in turn, may have adverse effect on the

---

prognosis.

Recently, low skeletal muscle mass (sarcopenia) has been proposed as part of the cancer cachexia syndrome [4]. Inflammatory cascades evoked by cytokines such as tumor necrosis factor (TNF)-α is considered as a major biological process in cachexia or sarcopenia as it can enhance anorexia, catabolism, and oxidative stress [5,6]. Sarcopenia, as a systemic marker of a relatively advanced stage in cancer progression, is found to be a novel predictor for impaired survival in cancer patients, including HCC [7]. Impaired homeostasis and unfavorable status of sarcopenia patients are also believed to be responsible for their poor outcomes. However, scarcely few studies have ever reported the mechanisms involved in the crosstalk between sarcopenia and HCC.

Chitinase-3 like-protein-1 (CHI3L1), a member of glycoside hydrolase family 18 including chitinases and non-enzymatic chitinase-like proteins, is a secreted molecule that plays an important role in cancer development, inflammatory diseases and oxidant injury via various mechanisms [8]. Emerging evidence has shown that CHI3L1 is overexpressed in many human cancer types and could promote cancer cell growth, proliferation, invasion and metastasis [9-11]. A particular property of CHI3L1 is the ability to induce reactive oxygen species (ROS) and lipid accumulation [12,13]. Increased lipid biosynthesis and excessive ROS accumulation are commonly observed in cancers including HCC, resulting in an increase in lipid peroxide (LPO). ROS-induced LPO has long been reported to participate in tumorigenesis [14,15]. LPO can induce DNA mutations, alter the cell growth and cell apoptosis, thus affect angiogenesis, inflammation and cancer progression [16].

In this setting, plasma metabolomics and inflammatory cytokine profiling were performed on 136 male HCC patients to identify the key signaling pathways. Tumor tissue RNA sequencing data and targeted oxylipin profiling were also enrolled. Through integrated analysis of multi-omics data, we successfully identified a cellular and molecular network in those HCC patients enduring sarcopenia.

2. Materials and methods

2.1. Patients

We collected the data including demographics, body mass index (BMI), preoperative lipid profiles (total cholesterol, total glyceride, high density lipoprotein and low density lipoprotein), α-fetoprotein (AFP) level, morphological features (tumor size, number of nodules), tumor differentiation, and vascular invasion for analysis. Routinely performed preoperative abdominal CT scan images closest to the transplantation date (within 1 month) were collected. The cross sectional skeletal muscle area should be measured at the level of the third lumbar vertebra (L3) using ImageJ [17]. This area was corrected for a patient's height, resulting in the L3-muscle index (cm^2/m^2), that is, skeletal muscle index (SMI).

The post-transplant patients were routinely followed up at the outpatient clinic. Disease progression was monitored by AFP, ultrasonography, and computed tomography every 3 months for the first 2 years and semiannually thereafter. Imaging evidence of either intrahepatic or extra-hepatic lesions was required for the diagnosis of tumor recurrence. A simple increase in AFP was insufficient. The average follow-up length is 41.3 months.

Compared with western countries, China has a much heavier HCC burden. Patients with early-stage HCC will usually undergo hepatectomy for cure, and liver transplantation is performed on patients with relatively advanced HCC in China. Therefore, the recurrence rate is also higher compared with western countries. To control the recurrence rate, efforts are being made to optimize candidate selection for HCC patients in China. For example, in Zhejiang province, the Hangzhou criteria is enrolled in governmental regulations, and recipients exceeding the Hangzhou criteria will not receive medical insurance for transplantation.

All of the liver grafts were obtained from donation after cardiac death. Informed consent was obtained from all the patients, and the study protocol was also approved by the Human Ethics Committee of our hospital. None of the liver grafts were acquired from executed prisoners.

2.2. Inflammatory cytokine profiling

We detected 37 inflammatory cytokines using Bio-Plex Pro™ Human Inflammation Panel 1, 37-Plex (Catalog No. 171AL001 M, Bio-Rad, US) according to the instruction manual. The plasma IL-6 level and TNF-α level were detected by Human IL-6 ELISA Kit (Catalog No. 1110602, Dakewe, China) and Human TNF-α ELISA Kit (Catalog No. 1117202, Dakewe, China), respectively.

2.3. Metabolomics

Plasma sample Liquid Chromatography Mass Spectrometry (LC-MS) was performed in Lu-Ming Biotech (Shanghai, China) as previously described [18]. The acquired LC-MS raw data were analyzed by the progqenesis QI software (Waters Corporation , Milford, USA) using the following parameters. Precursor tolerance was set 5 ppm, fragment tolerance was set 10 ppm, and retention time (RT) tolerance was set 0.02 min. Internal standard detection parameters were deselected for peak RT alignment, isotopic peaks were excluded for analysis, and noise elimination level was set at 10.00, minimum intensity was set to 15% of base peak intensity. The Excel file was obtained with three dimension data sets including *m/z*, peak RT and peak intensities, and RT–m/z pairs were used as the identifier for each ion. The resulting matrix was further reduced by removing any peaks with missing value (ion intensity = 0) in more than 50% samples. The internal standard was used for data QC (reproducibility). Metabolites were identified based on public databases including http://www.hmdb.ca/, http://www.lipidmaps.org/and self-built databases by Lu-Ming Biotech.

Targeted profiling on 12 metabolites in the cholesterol metabolism pathway was also performed in Lu-Ming Biotech (Shanghai, China). Meanwhile, Targeted oxylipin profiling was performed and analyzed in Metware Biotech (Wuhan, China) as previously described [19].

2.4. RNA sequencing

RNA sequencing was performed by Novogene (Beijing, China) as previously described [20]. Raw data (raw reads) of fastq format were firstly processed through in-house perl scripts. In this step, clean data (clean reads) was obtained by removing reads containing adapter, reads containing ploy-N and low quality reads from raw data. At the same time, Q20, Q30 and GC content the clean data were calculated. All the downstream analyses were based on the clean data with high quality. featureCounts v1.5.0-p3 was used to count the reads numbers mapped to each gene. And then FPKM of each gene was calculated based on the length of the gene and reads count mapped to this gene. FPKM, expected number of Fragments Per Kilobase of transcript sequence per Millions base pairs sequenced, considers the effect of sequencing depth and gene length for the reads count at the same time, and is currently the most commonly used method for estimating gene expression levels.

2.5. Cell culture, transfection and lentivirus infection

Mouse and human HCC cell lines (Hep1-6, Huh-7) and mouse myoblast cell lines (C2C12) were purchased from Shanghai Institute of Cell Biology, Chinese Academy of Sciences. The authenticity of all cells was verified by short-tandem repeat (STR) profiling. The maturation of muscle fibers in vitro was achieved by treating the C2C12 cells with horse serum at the concentration of 2% on the 2nd day after seeding.

The siRNAs, plasmids and lentiviral particles with GFP coding sequence were constructed by GenePharma (Shanghai, China). Lipofectamine 3000 transfection reagent was used for transient siRNA and

plasmid transfections following manufacturer's protocol (Invitrogen). Lentiviral particle infection was performed according to the previously described procedures [21]. The stable expression cells were selected with 5 μg/mL puromycin (Solarbio).

2.6. Colony formation assay

Pretreated Hep1-6 cells were seeded onto 6-well plates at a density of 2000 cells per well. After an incubation period of 14 days, the cells were fixed with methanol for 15 min and then stained with 0.1% crystal violet for 15 min. The experiments were performed in independent triplicates.

2.7. Cell Counting Kit-8 assay

Cell proliferation was detected using the Cell Counting Kit-8 (Catalog No. HY-K0301, MedChem Express, USA) assay. Briefly, pretreated HCC cells were placed in 96-well plates (normally 2000 cells per well) and cultured for 48 h. The results were measured at 450 nm using Absorbance Reader (BIO-TEK ELX800) at 0, 24, 48 and 72 h after adherence, respectively.

2.8. Cell migration/invasion assays

$3*10^4$-$5*10^4$ HCC cells were suspended in 200 μl serum-free medium with 0.1% BSA and loaded onto the upper compartment of chamber that contained a polycarbonate membrane (Corning Incorporated). For the invasion assays, the membrane of chamber shall be loaded with 30 μl of Matrigel at a concentration of 1 mg/ml, and incubated at a temperature of 37 °C for 4 h before cell loading. The serum concentration in lower compartment was 20%. After 48h incubation, the cells penetrating through the membrane were stained by crystal violet. The experiments were repeated independently three times.

2.9. Quantitative real-time PCR

Total RNA was extracted using MolPure® TRIeasy Plus Total RNA Kit (Catalog No. 19211ES60, YEASEN, China). RNA concentration was measured by Nanodrop (Thermo ScientificTM, USA), and each paired sample was adjusted to the same concentration. For reverse transcription (RT), we used an RT reagent kit purchased from Vazyme (Catalog No. R323-01, China). Real-time PCR was subsequently performed using SYBR Premix supplied by Vazyme (Catalog No. Q711-02, China) on the Applied Biosystems Quantstudio 5 and Quantstudio 6 Flex (Thermo Fisher, USA). The primers were synthesized by Tsingke (China), and the following primer sequences were used:

Gapdh-F: 5′- AGGTCGGTGTGAACGGATTTG -3′
Gapdh-R: 5′- TATGGTTTTGACGACTGTGTGAT -3′
Chi3l1-F: 5′- CTGCGTACAAGCTGGTCTG -3′
Chi3l1-R: 5′- TGGATGGCGTCTGGTAAGAAG -3′

2.10. Western blotting

Cells were washed in ice-cold PBS, and then lysed in RIPA buffer. Western blotting was carried out as described previously [22]. The following antibodies were used in this study: anti-CHI3L1 (Catalog No. ab180569, 1:1000, Abcam, China), anti-Myogenin (Catalog No. ab124800, 1:1000, Abcam, China), anti-GAPDH (Catalog No. ab8245, 1:2000, Abcam, China), anti-TNFR1 (Catalog No. 21574-1-AP, 1:1000, Proteintech, China), anti-MMP2 (Catalog No. 10373-2-AP, 1:1000, Proteintech, China), anti-MMP9 (Catalog No. 10375-2-AP, 1:1000, Proteintech, China), anti-Vimentin (Catalog No. 5741T, 1:1000, Cell Signaling, China), anti-Snail (Catalog No. 3879T, 1:1000, Cell Signaling, China), anti-Cleaved Caspase3 (Catalog No. 9661S, 1:1000, Cell Signaling, China), anti-LRP1 (Catalog No. 10711-1-AP, 1:1000, Proteintech, China), anti-COX2 (Catalog No. 12375-1-AP, 1:1000, Proteintech, China), anti-LOX (Catalog No. 17958-1-AP, 1:1000,

Proteintech, China), anti-FASN (Catalog No. 3180S, 1:1000, Cell Signaling, China), anti-CPT1A (Catalog No. 12252S, 1:1000, Cell Signaling, China), anti-SREBP2 (Catalog No. ab30682, Abcam, China), and anti-β-actin (Catalog No. 60008-1-Ig, Proteintech, China).

2.11. Immunofluorescence

Cells were cultured on glass coverslips attached to 6-well plates. Appropriate fluorochrome-conjugated secondary antibodies were used to recognize target proteins. DAPI (300 nM) staining was applied for nuclear localization. The distribution of different fluorescence was monitored by Laser-scanning confocal microscope (Olympus). The following antibodies were used in this study: GP-39 (Catalog No. sc-393494, 1:500, Santa-Cruz, USA).

2.12. Cell apoptosis assay

Apoptosis was detected in C2C12 cells using an FITC Annexin V Apoptosis Detection Kit II (Dojindo). Apoptotic agents (LPS at a concentration of 5 μg/ml, Santa-cruz, US, Catalog No. sc3535) were introduced 48h prior to detection. Cells were analyzed using a flow cytometer (LSR II; BD Bioscience). All experiments were conducted in triplicate.

2.13. Oil red O

The pre-treated cells were removed, washed twice with PBS, fixed with 4% formaldehyde at room temperature, and washed three times with PBS. To stain the lipids, the cells or sections were treated with filtered Oil red O solution for 1 h at room temperature and washed twice with PBS. Red-stained lipid droplets were observed under a microscope. The assay is further repeated on cells cultured in mediums with 100umol/L fatty oil acid.

2.14. LPO detection

Cellular LPO level was detected using a lipid peroxidation assay kit (Catalog No. A106-1-2, Nanjing Jiancheng, China) according to the manure. LPO staining was accomplished using BODIPYtm 581/591 C11 (Lipid peroxidation sensor, Catalog No. thermo.3861, Invitrogen, US) according to the described procedures [23].

2.15. Measurement of mouse CHI3L1 concentration

The measurement of mouse CHI3L1 concentration in the cell culture medium and mouse ascites was performed using the Mouse CHI3L1 GENLISATM ELISA kit (KRISHGEN BioSystem, India, Catalog No. KLM1136).

2.16. Establishment of mouse cachectic model

We established liver cancer associated mouse cachectic model by intraperitoneal injection of H22 cells ($2*10^6$), and monitored mouse weight and grip power change. Referring to the previous study [24], cachexia model was established since day 7 after intraperitoneal injection. The mice were categorized into mild cachectic group (day 8 post-injection) and severe cachectic group (day 16 post-injection).

2.17. Statistical analysis

The Chi-square test was used for categorical variables and Student's *t*-test was used for continuous variables. Kaplan–Meier method was used for survival and recurrence-risk analysis by the log-rank test. Overall survival (OS) was calculated from the date of transplant to the date of death. The recurrence free survival (RFS) was calculated from the date of transplant to the date when tumor recurrence was diagnosed. And if recurrence was not diagnosed, the cases were censored at the date of

death or the last date of follow-up. The Cox proportional hazards regression (backward stepwise) was used to determine the independent factors for survival and recurrence. The statistical analyses and graph-drawing were performed by SPSS 19.0 (SPSS Inc., Chicago, IL, USA), R 4.0 (R Foundation, Vienna, Austria) and Cytoscape (The Cytoscape Consortium, San Diego, CA Version 3.8) Graphpad (GraphPad Software, LLC, San Diego, USA). A p value below 0.05 was considered statistically significant.

3. Results

3.1. Plasma omics profiling identified key cytokines and metabolic pathway

3.1.1. Sarcopenia in HCC

This study retrospectively profiled the pre-operative plasma sample of 155 HCC patients undergoing liver transplantation in the First Affiliated Hospital, Zhejiang University School of Medicine from April 2012 to December 2017. All of the tumors were pathologically confirmed to be HCC. Among them, 143 were males and 12 females. As the definition for sarcopenia is rather different for male and female patients, and the
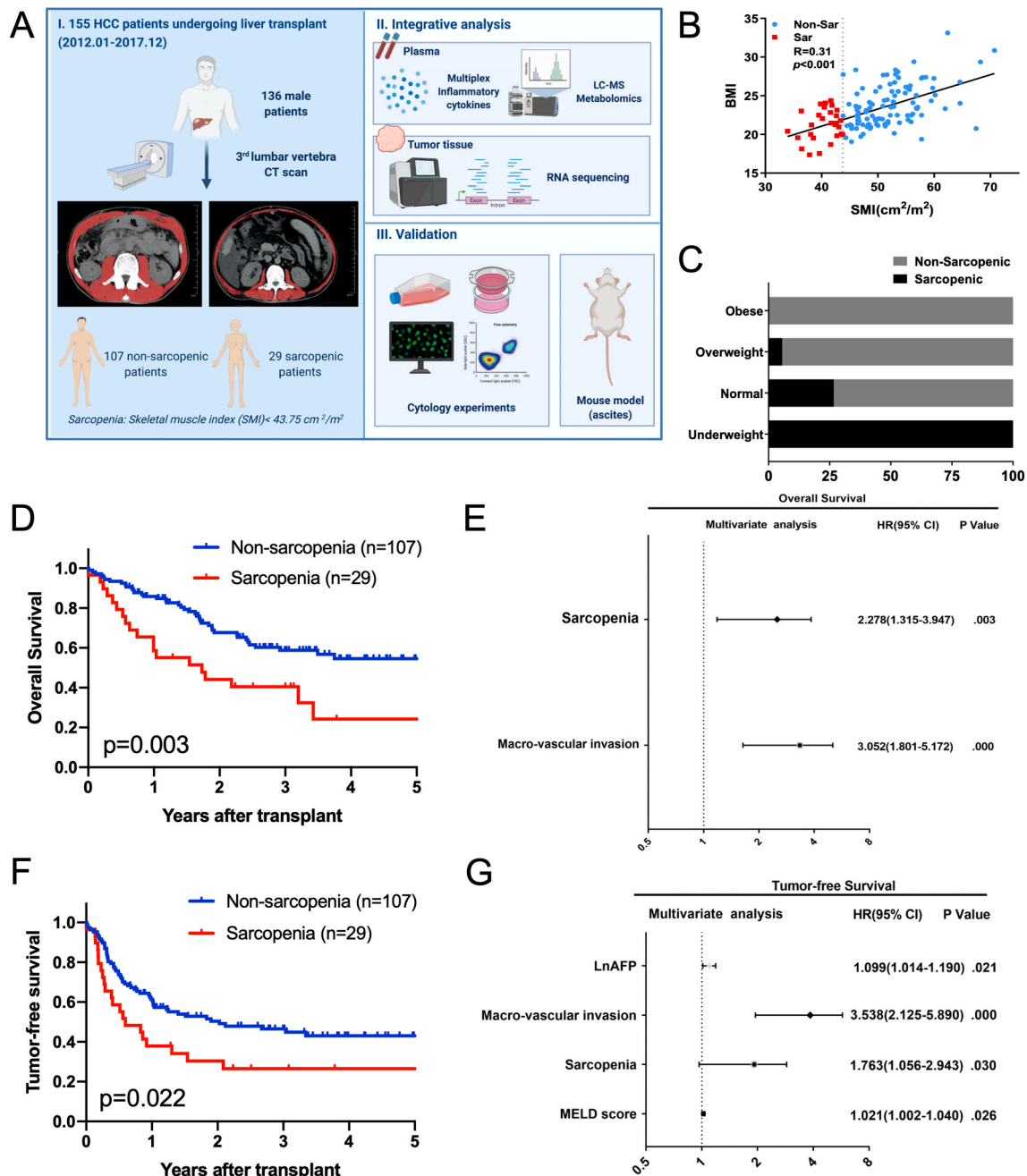
Fig. 1. General workflow and the clinical impact of sarcopenia. (A) The general workflow of the present study, and the cross sectional skeletal muscle image at the level of L3 vertebra from a non-sarcopenic patient and a sarcopenic patient; (B) SMI positively correlated with BMI (p < 0.001); (C) Incidence of sarcopenia decreased in the obese patients; (D) Sarcopenia is associated with impaired overall survival after liver transplantation for HCC (p = 0.003); (E) Multivariate analysis for overall survival after transplantation; (F) Sarcopenia is associated with impaired tumor-free survival after liver transplantation for HCC (p = 0.022); (G) Multivariate analysis for tumor-free survival after transplantation.

gender difference in inflammatory and metabolic status may disturb the reliability of the results, only the male patients were further analyzed in this study. After all, 136 male patients, with essential data completed, were enrolled for analysis. The general workflow of the study is listed as Fig. 1A.

According to the frequently reported cut-off value (43.75 cm^2/m^2) of SMI for hepatoma-related sarcopenia in men [25-27], the 136 patients were divided into the non-sarcopenic group (n = 107) and sarcopenic group (n = 29). And the representative L3 vertebra CT images were also shown in the workflow (Fig. 1A). As an index for nutritious status, SMI positively correlated with BMI (p < 0.001), and the incidence of sarcopenia decreased in the obese patients (Fig. 1B and C). By comparing between the non-sarcopenic group and sarcopenic group, the demographical indexes and clinical characteristics were generally comparable, except for the nutrition-related indexes (BMI and high-density lipoprotein, Supplementary Table S1). Univariate analysis for overall and tumor-free survival was shown in Supplementary Table S2. Sarcopenia was associated with impaired overall survival and tumor-free survival (p < 0.05, Fig. 1D and F). Multivariate analysis showed that sarcopenia was an independent predictor for both overall survival and tumor-free survival (p < 0.05, Fig. 1E and G). Therefore, Sarcopenia is associated with the outcomes of HCC patients.

3.1.2. Inflammatory cytokine and metabolomic profiling

The plasma TNF-α level was below detectable limit in more than half of the cases, and was thereby excluded from the current analysis. After all, 38 cytokines were enrolled for inflammatory cytokine profiling

(Fig. 2A). By comparing between the non-sarcopenic group and sarcopenic group, 9 cytokines were identified with significant difference (p < 0.05), and all of them were upregulated in sarcopenic patients, indicating a pro-inflammatory status in sarcopenia. Meanwhile, when we compared between the non-recurrent (n = 59, 9 patients died within 100 days after transplant without recurrence and were therefore excluded) and recurrent (n = 68) patients, 3 cytokines were decreased and 23 were up-regulated in the recurrent group (p < 0.05, Supplementary Fig. S1A). Similarly, by comparing the metabolomic profiling between the non-sarcopenic and sarcopenic patients, 321 metabolites were identified with significant difference (p < 0.05). Meanwhile, when we compared between the non-recurrent and recurrent patients, 618 metabolites were identified (p < 0.05, Supplementary Fig. S1B). Venn Diagram showed that 6 cytokines and 83 metabolites were concurrently related to sarcopenia and HCC recurrence risk (Fig. 2B).

The identified 6 cytokines were CHI3L1, sTNF-R1, IFN-β, IL12 (p40), IL26 and TNFSF13B. The protein interaction mapping showed co-expression relation among these cytokines and the predicted interaction (Fig. 2C). The heatmap for the 83 metabolites was shown in Fig. 2D. Pathway analysis showed that these metabolites were majorly related to lipid metabolism, including sterol lipids, fatty acyl et al. (Fig. 2E). Among them, the metabolites belonging to sterol metabolism were generally decreased in sarcopenia (Fig. 2F). On the other hand, the metabolites belonging to fatty acid metabolism were also generally decreased, however, a metabolite of the lipoxidation cascades, N-acetyl-LTE4, was significantly increased (Fig. 2G).
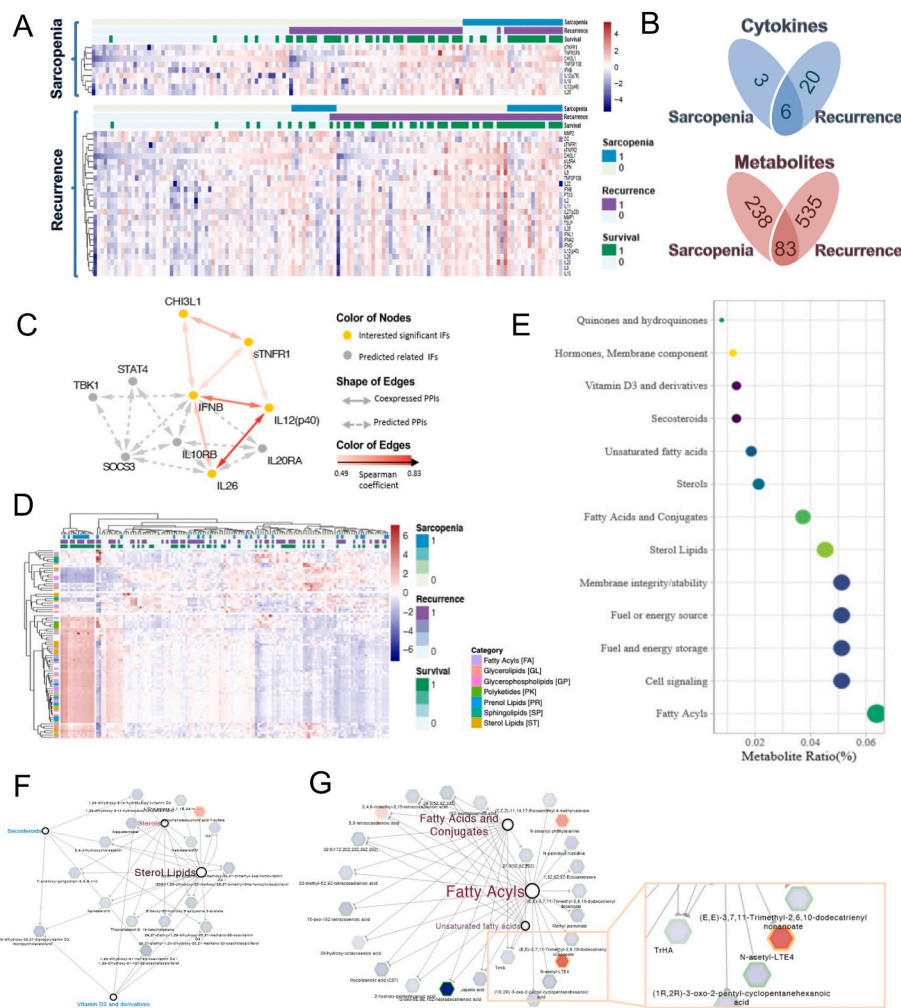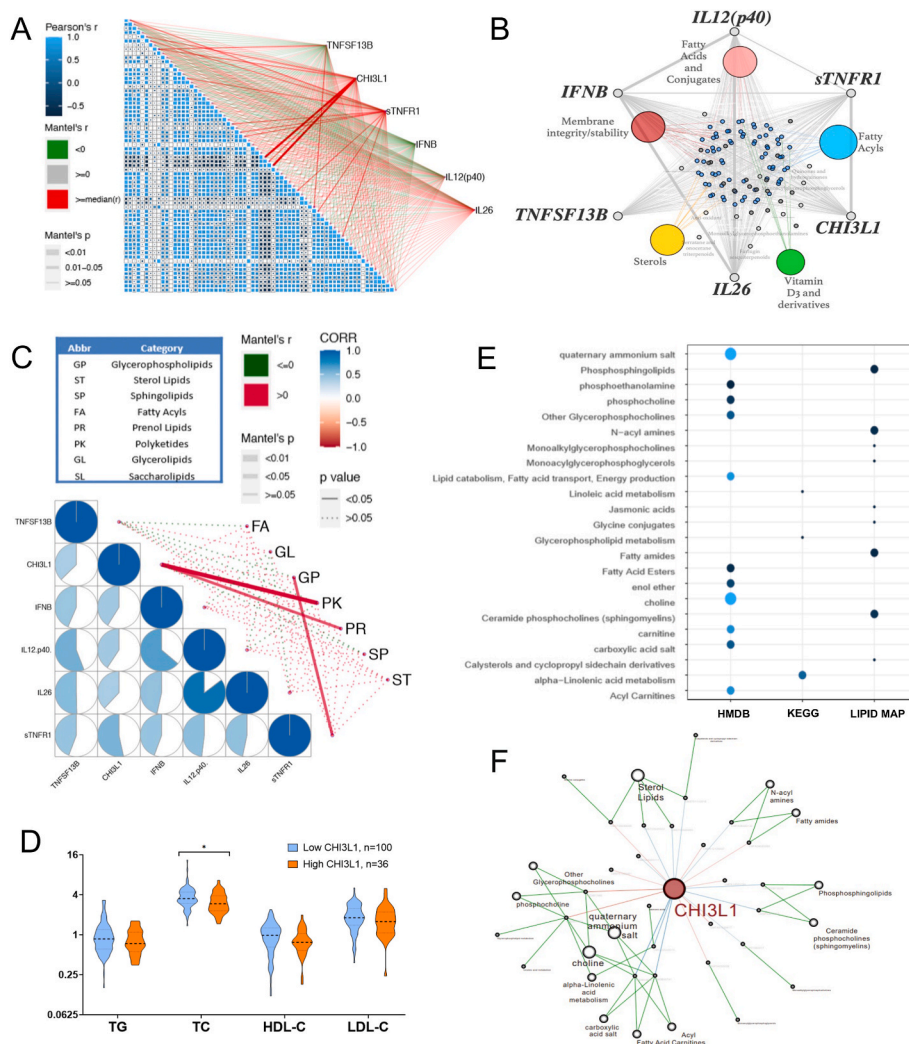

Fig. 2. Inflammatory cytokine and metabolomic profiling. (A) Heatmaps for the differential cytokines related to sarcopenia and tumor recurrence, respectively (R package: ggplot2); (B) The Venn Diagrams for the cytokines/metabolites related to sarcopenia and tumor recurrence concurrently; (C) The protein interaction mapping for the 6 cytokines that were concurrently related to sarcopenia and tumor recurrence; (D) The heatmap for the metabolites that were concurrently related to sarcopenia and tumor recurrence (R package: ggplot2); (E) Pathway analysis for the identified metabolites that were concurrently related to sarcopenia and tumor recurrence (MBROLE 2.0); (F) and (G) The co-expression network of the metabolites belonging to sterol metabolism and fatty acid metabolism. Gray hexagon and green border indicate decreased level in sarcopenic patients and recurrent patients, respectively. Red hexagon and orange border indicate increased level in sarcopenic patients and recurrent patients, respectively. (For interpretation of the references to colour in this figure legend, the reader is referred to the Web version of this article.)

3.1.3. Integrated analysis of cytokine and metabolomics profiling

We further analyzed the connections between the identified cytokines and metabolites. CHI3L1 and sTNF-R1 were the major 2 cytokines that were significantly related to the metabolites, especially for fatty acid metabolism (Fig. 3A and B). Shown in Fig. 3C, CHI3L1 and sTNF-R1 were significantly related to prenol lipid and glycerophospholipid metabolism, respectively (LIPID MAPS® Classification System, Main Class).

CHI3L1 and sTNF-R1 were therefore further analyzed in this study. Increased plasma CHI3L1 and sTNF-R1 levels were both associated with poor overall and tumor-free survival (p < 0.05, Supplementary Figs. S2A–S2D). They were both linearly related to SMI (p < 0.05, Supplementary Fig. S2E). We also analyzed their connections with clinical lipid profiles. Interestingly, CHI3L1 was negatively related to total cholesterol level and HDL level (p < 0.05, Fig. 3D and Supplementary Fig. S2F). Then we analyzed the plasma metabolites that were linearly related to plasma CHI3L1. Pathway enrichment and co-expression network showed that CHI3L1 was mostly related to fatty acid metabolism, including fatty acid ester, fatty amide, linolenic acid metabolism, and carnitine (Fig. 3E and F). Steroid lipids were also related.
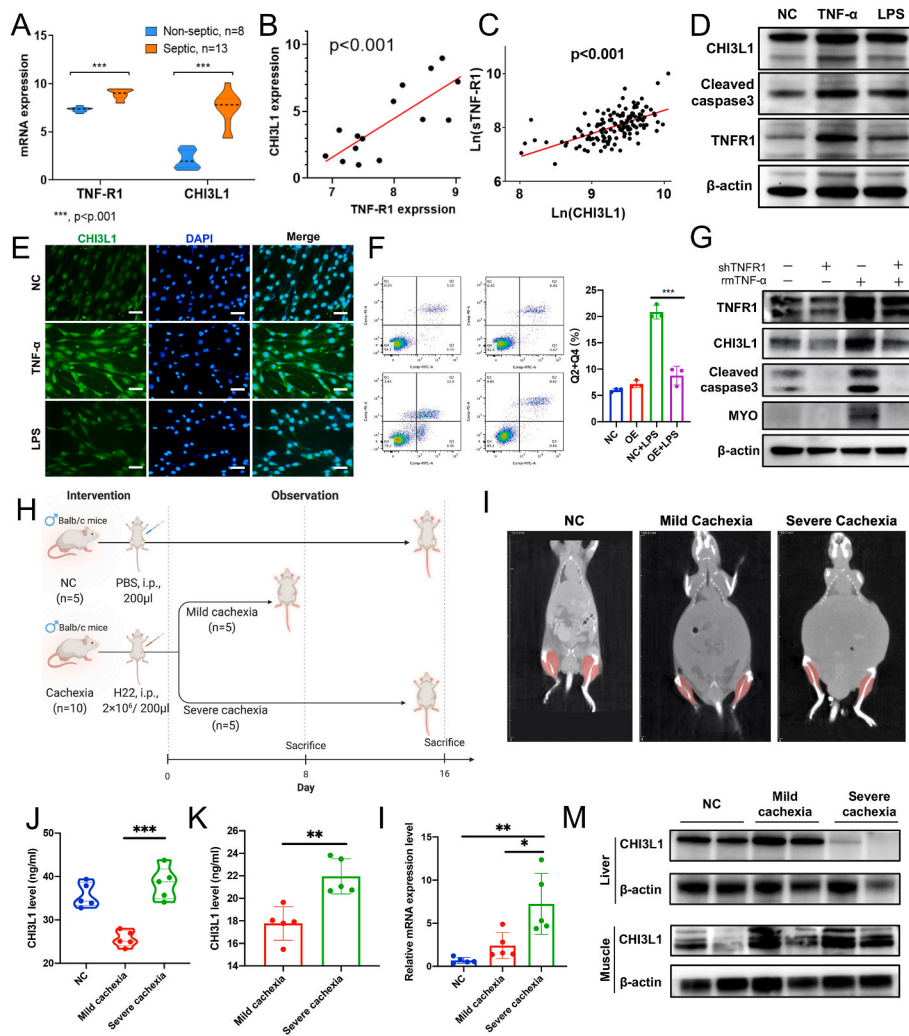
3.2. CHI3L1 is induced to protects muscle cell against inflammatory damage

3.2.1. CHI3L1 promotes C2C12 myoblast cell maturation

In vitro, CHI3L1 level increased along with the maturation of the C2C12 myoblast cells after treatment with horse serum (Supplementary Figs. S3A–3C). And over-expression of CHI3L1 promoted the proliferation of C2C12 muscle cells (Supplemental Fig. S3D). Stable over-expression and knockdown of CHI3L1 showed that CHI3L1 promoted the maturation of C2C12 muscle cells, that is, morphologically more like muscle fibers at day 4 (Supplementary Fig. S3E).

3.2.2. Muscle CHI3L1 and TNF-R1 are up-regulated in systemic inflammation

We analyzed an online transcriptome dataset of skeletal muscle biopsy tissues from 21 patients in ICU, including 8 non-septic cases and 13 septic cases (GDS3463) [28]. We found that CHI3L1 and TNF-R1 mRNA in the skeletal muscle was significantly upregulated in septic patients, that is, under systemic inflammatory circumstances (Fig. 4A). Moreover, TNF-R1 expression positively correlated with CHI3L1 (Fig. 4B). In our own patient cohort, plasma CHI3L1 and sTNF-R1 were also linearly correlated (Fig. 4C). We thereby speculated that CHI3L1 and TNF-R1 interacts with each other under inflammatory circumstances.

Fig. 3. Integrated analysis of cytokine and metabolomics profiling. (A) The corrplot for the identified 83 metabolites and their relations to the 6 identified cytokines (R package: ggcor); (B) Co-expression network in between the identified metabolites and the cytokines; (C) The corrplot for the identified 6 cytokines and their relations to the major metabolic categories (R package: ggcor); (D) Elevated plasma CHI3L1 was associated with decreased serum total cholesterol level; (E) and (F) Pathway enrichment and co-expression network for the metabolites linearly related to plasma CHI3L1.

Fig. 4. CHI3L1 is upregulated to protect muscle cells against inflammatory damage. (A) and (B) CHI3L1 and TNF-R1 mRNA is significantly upregulated in the skeletal muscle tissues of septic patient. And TNF-R1 mRNA level is positively related to CHI3L1 mRNA (GDS3463); (C) Plasma CHI3L1 and sTNF-R1 were linearly correlated in our patient cohort; (D) and (E) TNF-α or LPS treatment can increase the expression of CHI3L1 in C2C12 cells (scale bar, 50 μm); (F) CHI3L1 overexpression inhibited LPS-induced C2C12 cell apoptosis; (G) Knockdown of TNF-R1 in the C2C12 cells can efficiently inhibit TNF-α-induced CHI3L1 up-regulation, as well as cleaved caspase 3, MYO, Myogenin; (H) Establishment of mouse cachetic models by intraperitoneal injection of H22 cells; (I) The CT of mouse cachetic models; (J) and (K) CHI3L1 level was significantly elevated in the plasma and ascites of severe cachexia (p < 0.05); (L) and (M) CHI3L1 level was significantly elevated in in the muscle tissues of cachetic mice. Data represent the mean ± SD. *P < 0.05, **P < 0.01, ***P < 0.001.

3.2.3. CHI3L1 is induced to protect muscle cell against inflammatory damage in a TNF-R1 dependent manner

TNF-α (20 mg/ml) or lipopolysaccharide (LPS, 2.5 μg/ml) treatment can increase the expression of CHI3L1 in C2C12 cells (Fig. 4D and E). For the apoptosis assay, we used LPS as the inflammatory stimulation agent to induce sufficient apoptosis. The results showed that the upregulation of CHI3L1 inhibited LPS-induced C2C12 cell apoptosis (Fig. 4F), while TNF-R1 overexpression promoted LPS-induced C2C12 cell apoptosis (Supplementary Fig. S3F).

We speculated that CHI3L1 is upregulated by the activation of TNF-R1 under inflammatory condition. Thus, TNF-α was used to activate TNF-R1. Knockdown of TNF-R1 in the C2C12 cells can efficiently inhibit TNF-α-induced CHI3L1 up-regulation, as well as cleaved Caspase 3 (Fig. 4G). Therefore, CHI3L1 is induced to protect muscle cell against inflammatory damage in a TNF-R1 dependent manner.

3.2.4. CHI3L1 is elevated in the skeletal muscle and circulation of cachectic mice

We enrolled another online transcriptome dataset of skeletal muscle tissue from CD2F1 mice with subcutaneous xenograft of C26 cells (GSE24112) [29]. The dataset contains 4 normal controls, 3 cases of early cachexia (weight loss = 10%), and 4 cases of severe cachexia (weight loss>10%). Interestingly, we found significantly up-regulated CHI3L1 and TNF-R1 mRNA level in the muscle tissues of cachectic mice, especially in the severe cases (Supplementary Fig. S4A and S4B). And CHI3L1 and TNF-R1 mRNA level were linearly correlated

(Supplementary Fig. S4C).

To confirm the results in liver cancer, we also established mouse mild and severe cachectic models by intraperitoneal injection of H22 cells (Fig. 4H). The CT images of different groups were shown in Fig. 4I. The weight loss and ascites volume were confirmed the cachectic status, especially the severe group (Supplementary Fig. S4D and 4E). And the grip strength declined along with prolonged duration of tumor bearing (Supplementary Fig. S4F). CHI3L1 level was significantly elevated in the plasma and ascites in severe cachexia (p < 0.05, Fig. 4J and K). Western and PCR results showed that CHI3L1 level was significantly elevated in in the muscle tissues of cachectic mice, but not in the livers of severe cachectic mice (Fig. 4L and M). Therefore, CHI3L1 is elevated in the skeletal muscle and circulation in cachexia.

3.3. CHI3L1 promotes HCC progression in an LPO-dependent manner

3.3.1. CHI3L1 expressed by the muscle cells promotes HCC progression

Over-expression of CHI3L1 by plasmid promoted Hep1-6 cell proliferation (Fig. 5A). Over-expression of CHI3L1 by lentivirus promoted Hep1-6 HCC cell colony formation, while its down-regulation had the opposite effect (Fig. 5B). Moreover, CHI3L1 showed potent pro-invasive effects in Hep1-6 cell (Fig. 5C and Supplementary Fig. S5A). Aforementioned pro-cancerous phenotypes including proliferation, colony formation, invasion and migration were also observed in Huh7 cells (Supplementary Figs. S5B–S5D). WB results showed that overexpression of CHI3L1 could promote the expression of invasion-related proteins
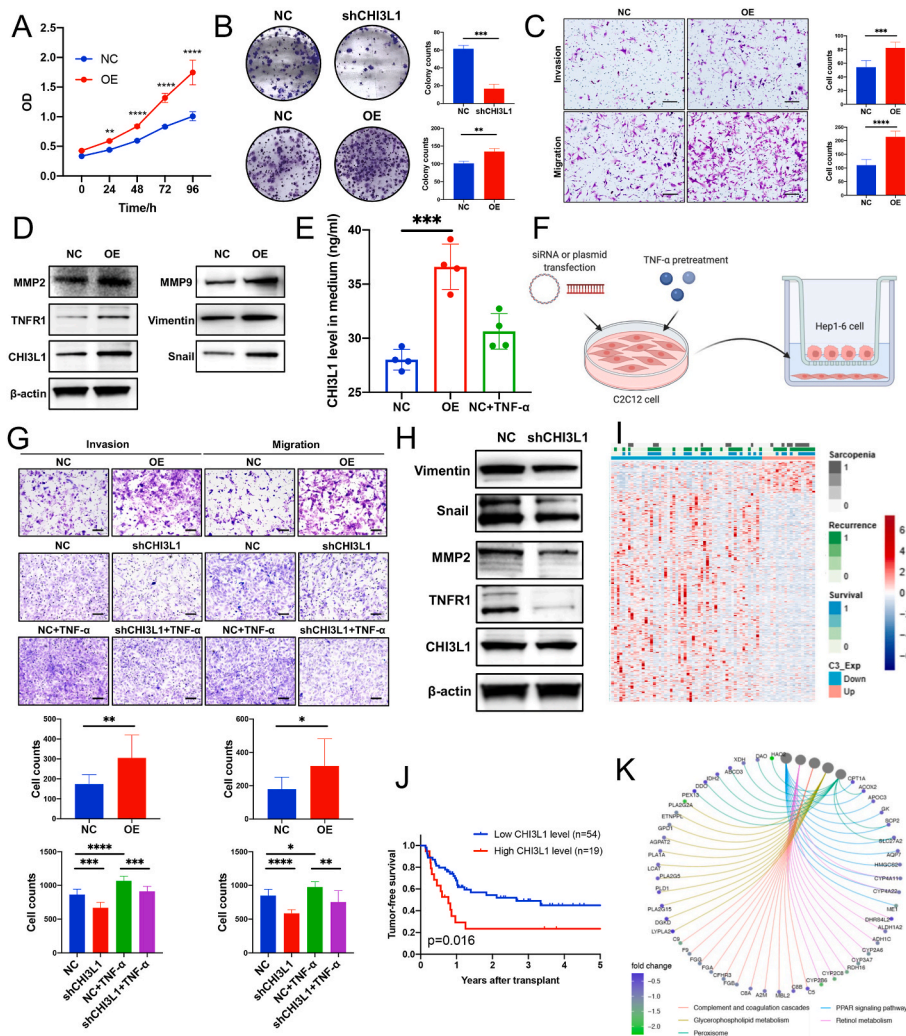
Fig. 5. CHI3L1 promotes cancer cell metastasis. (A) CHI3L1 over-expression promoted Hep1-6 cell proliferation; (B) CHI3L1 stable over-expression promoted Hep1-6 cell colony formation, while its stable down-regulation had opposite effects; (C) CHI3L1 over-expression promoted Hep1-6 cell invasion and migration (scale bar, 200 μm); (D) the overexpression of CHI3L1 can promote the expression of invasion-related proteins such as MMP2, MMP9, etc.; (E) CHI3L1 level was increased in the medium of myoblasts with CHI3L1 over-expression; (F) The schematic diagram for the co-culture model in the transwell chamber; (G) CHI3L1 over-expression in the myoblasts promotes the invasion and migration of Hep1-6 cells. On the other hand, TNF-α pre-treatments on the myoblasts can also promote the invasion and migration of Hep1-6 cells, and the effect can be alleviated by CHI3L1 knockdown in the myoblasts (scale bar, 100 μm); (H) Co-culture with CHI3L1 knockdown C2C12 cells can suppress the expression of invasion-related proteins such as MMP2, Vimentin, etc. in Hep1-6 cells. (I) We performed RNA sequencing on the tumor tissues of 73 out of the 136 patients. The heatmap for the differentially expressed genes in regards to plasma CHI3L1 level; (J) Plasma CHI3L1 was related to tumor-free survival after transplantation (p = 0.016); (K) Enrichment analysis of the different expressed genes in regards to plasma CHI3L1 (R package: clusterProfiler). Data represent the mean ± SD. *P < 0.05, **P < 0.01, ***P < 0.001, ****P < 0.0001.

such as MMP2 (Fig. 5D).

Meanwhile, we also detected elevated CHI3L1 in the medium of CHI3L1 over-expressing C2C12 cells or TNF-α-treated C2C12 cells (Fig. 5E). It proved that CHI3L1 is a secretory protein and can be secreted under the stimulation of TNF-α. We then co-cultured the pre-treated myoblasts with Hep1-6 cells in transwell chambers (Fig. 5F). CHI3L1 over-expression in the myoblasts promotes the invasion and migration of co-cultured Hep1-6 cells. On the other hand, TNF-α pre-treatments on the myoblasts can also promote the invasion and migration of Hep1-6 cells, and the effect can be alleviated by CHI3L1 knockdown in the myoblasts (Fig. 5G). WB results also showed that co-culture with CHI3L1 knockdown C2C12 cells could suppress the expression of invasion-related proteins such as MMP2 in Hep1-6 cells (Fig. 5H). The above results showed that CHI3L1 secreted by the muscle cells promotes the invasion of co-cultured HCC cells.

### 3.3.2. Pathway analysis related to plasma CHI3L1

We performed RNA sequencing on the tumor tissues of 73 out of the 136 patients (Fig. 5I). In this cohort, plasma CHI3L1 was still related to tumor-free survival (p = 0.016, Fig. 5J), but tumor CHI3L1 mRNA level was not (p > 0.05). Moreover, plasma CHI3L1 was significantly related to SMI (p = 0.008), but was not significantly associated with CHI3L1 mRNA level in the HCC tissues (p = 0.063, Supplementary Fig. S6A), indicating that the plasma CHI3L1 is closely related to muscle wasting but not tumor itself. We further analyzed the transcriptome data together with the plasma CHI3L1 level. The heatmap and volcano plot

were shown in Fig. 5K and Supplementary Fig. S6B. The differently expressed genes associated with plasma CHI3L1 were related to PPAR signaling, peroxisome, glycerophospholipid metabolism pathway and arachidonic acid (AA) metabolism (Fig. 5K and Supplementary Fig. S6C). All the above-mentioned pathways are critical for fatty acid metabolism. For instance, 11 genes in the PPAR signaling pathway, which is responsible for fatty acid degradation, were down-regulated.

3.3.3. CHI3L1 promotes LPO accumulation, which accelerates HCC progression

We further enrolled the analysis results of the transcriptome data comparing CHI3L1 over-expressing cells and control cells in 2 different human HCC cell lines [30], and observed alteration in cellular oxidative pathways (Supplementary Fig. S7A). Meanwhile, we also identified increased ROS level in CHI3L1 over-expressing Hep1-6 cells compared to the negative control cells (Fig. 6A). We therefore concluded that CHI3L1 promotes oxidative stress in liver cancer cells.

As pathway analysis showed that CHI3L1 may disturb lipid metabolism, we performed oil red staining assay on the Hep1-6 cells, and found that CHI3L1 promoted lipid accumulation, especially in the medium with high fatty acid (Fig. 6B). We hypothesized that fatty acid might be accumulated and peroxidized by the excess ROS, and thereby performed LPO staining assay on the Hep1-6 cells. Increased LPO accumulation was observed in the CHI3L1 over-expressing cells, especially in the medium with high fatty acid (Fig. 6C). LPO detection kit also showed that the LPO level was increased in CHI3L1 over-expressing
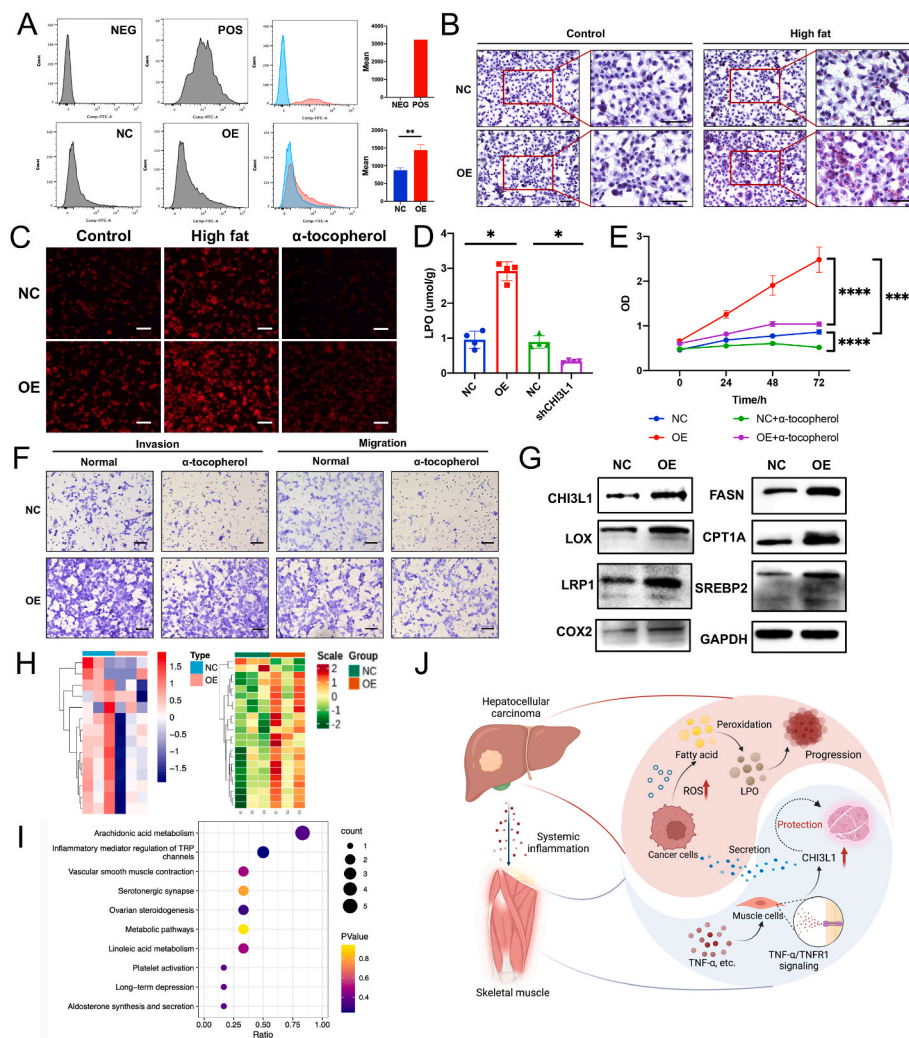
Fig. 6. CHI3L1 promotes HCC progression by disturbing LPO metabolism. (A) CHI3L1 overexpression increased the cellular ROS level in Hep1-6 cells; (B) CHI3L1 promoted fat accumulation in Hep1-6 cells, especially in high fatty acid (HF) medium (scale bar, 100 μm); (C) LPO staining assay on the Hep1-6 cells identified increased LPO accumulation in the CHI3L1 over-expressing cells, especially in high fat medium. Tocopherol inhibited LPO synthesis in the Hep1-6 cells; (D) LPO detection kit showed increased LPO level in CHI3L1 over-expressing Hep1-6 cells and decreased LPO level in CHI3L1 knockdown Hep1-6 cells; (E) LPO inhibition using α-tocopherol can compromise pro-proliferative effects of CHI3L1 in Hep1-6 cells; (F) LPO inhibition can compromise pro-invasive and migrative effects of CHI3L1 in Hep1-6 cells (scale bar, 200 μm); (G) The lipid peroxidation enzymes including LOX and COX2 were up-regulated in the CHI3L1 over-expressing Hep1-6 cells; (H) Targeted profiling on 14 metabolites in the cholesterol metabolism pathway showed that they were generally down-regulated by CHI3L1 (negative control vs CHI3L1 over expression, repeats = 3). Targeted profiling of 71 oxylipins identified 22 differential oxylipins, including 20 up-regulated and 2 down-regulated by CHI3L1 (negative control vs CHI3L1 over expression, repeats = 3); (I) Pathway analysis showed that CHI3L1 altered the level of 5 metabolites in arachidonic acid metabolism pathway in the Hep1-6 cells; (J) The schematic diagram. Data represent the mean ± SD. *P < 0.05, **P < 0.01, ****P < 0.0001.

cells, while decreased in CHI3L1 knockdown cells (Fig. 6D). We used α-tocopherol, an antioxidant for polyunsaturated lipids, at a concentration of 200 μmol/L (T3376, Sigma). α-tocopherol inhibited Hep1-6 tumor cell proliferation, invasion and migration, and substantially compromised the pro-cancerous effects of CHI3L1 (Fig. 6E and F).

We further find that the lipid oxidation enzymes including LOX and COX2 were up-regulated in the CHI3L1 over-expressing Hep1-6 cells (Fig. 6G). We also performed targeted profiling of 14 key metabolites in the cholesterol metabolism pathway and 71 oxylipins on the Hep1-6 cells (Control vs Over-expression, repeats = 3, Fig. 6H). The cholesterols were generally decreased by CHI3L1 (Supplementary Fig. S7B). Meanwhile, we identified 22 differential oxylipins (VIP value > 1 and fold change>2), including 20 up-regulated and 2 down-regulated (Supplementary Fig. S7C). After excluding oxylipins without annotation of KEGG database, pathway analysis showed that 5 out of 6 oxylipins, that is, AA, 15-HETE, 15-oxoETE, 5-oxoETE and 8,9-EET, were related to AA metabolism pathway (Fig. 6I), and they were all up-regulated by CHI3L1.

4. Discussion

Sarcopenia has been frequently reported to be associated with increased morbidity and mortality in various diseases, especially for cancers [31-33]. Previous studies proved the close relation between sarcopenia and HCC [34-36], but few of them investigated the molecular and cellular crosstalk in between. Sarcopenia reflects the systemic

nutritious and metabolic condition. It is usually accompanied by systemic inflammation [37]. It is speculated that sarcopenia-related systemic inflammation and metabolic disorders might affect the outcomes of cancer. According to the results of the multi-omics profiling, the pro-inflammatory cytokines, CHI3L1 and sTNF-R1, and a series of metabolites in lipid metabolism pathway, may participate in the interactions between the sarcopenia and HCC.

CHI3L1 has been revealed as important regulator in liver cancer progression. Pan et al. found that CHI3L1 is increased in HCC cells compared to tumor-adjacent cells, and will further increase in metastatic HCC [38]. CHI3L1 promoted cancer cell invasion and metastasis by activating the EMT pathways [30]. In our study, we identified elevated plasma CHI3L1 level as a risk factor for tumor recurrence, while cellular CHI3L1 promotes cancer progression in vitro. However, what is interesting about our results is that, elevated CHI3L1 was also observed in those HCC patients with sarcopenia. In our mouse cachectic models, we observed elevated CHI3L1 in the plasma and ascites of mice with severe cachexia, proving that CHI3L1 is elevated in the circulation system under severe cachexia. Therefore, we speculated that it may be a key regulator in HCC-related sarcopenia.

A previous study has found that CHI3L1 is an auto-protective factor that is stimulated to protect skeletal muscle cells against TNF-α [39]. Interestingly, we also identified up-regulated sTNF-R1, along with CHI3L1, as related to sarcopenia and recurrence risk concurrently. And they were the 2 key cytokines that were closely related to metabolic changes. sTNF-R1 is the secreted version of TNF-R1. By analyzing the

GEO data, we found increased expression of CHI3L1 and TNFR1 in the skeletal muscle of both septic ICU patients and cachectic mouse. In our own HCC-related cachectic models, we confirmed the elevation of CHI3L1 level in the atrophic muscle tissue. Our in vitro study further showed that CHI3L1 is up-regulated and secreted through the TNF-α/TNF-R1 pathway, so as to protect muscle cells against inflammatory damage.

Moreover, we also observed dysregulated lipid metabolism as related to sarcopenia and recurrence risk concurrently. We firstly found that the majority of sterol lipids and fatty acyls were decreased in patients with sarcopenia and high recurrence risk, indicating a mal-nutritious status. CHI3L1 is an important marker in diseases with lipid disorders [12], and we observed that plasma CHI3L1 level negatively correlates with total cholesterol, so we speculated that the change in lipid metabolism may be somehow regulated by CHI3L1. Therefore, we performed targeted profiling on the cholesterol metabolism pathway, and found that cholesterol metabolites were generally decreased in HCC cells over-expressing CHI3L1. Our results suggested that CHI3L1 can significantly inhibit cholesterol metabolism in the HCC patients with sarcopenia.

Similar to the sterol lipids, the majority of fatty acyls were decreased in patients with sarcopenia and high recurrence risk. However, LTE4, a metabolite of AA pathway, was increased. By interpreting the tumor tissue RNA sequencing data, we found CHI3L1 is most closely related to fatty acid metabolism and oxidative stress. Lipid accumulation, oxidative stress, and concomitant lipid peroxidation are linked to cancer initiation and progression. Several studies have reported that increased level of LPO products is significantly related to growth and metastasis of cancer including colon and liver cancers [40-42], while the utilization of antioxidants could protect against oxidation stress and rescue tumorigenic phenotypes [43]. Further, some LPO like 4-HNE were shown to upregulate the expression of transcription factors such as nuclear factor-κ-gene binding (NF-κB), and activate the c-Jun N-terminal kinase (JNK)/c-Jun pathway and Kelch ECH associating protein 1 (KEAP1)/nuclear factor erythroid 2-related factor 2 (NRF2) pathway [44,45]. In our study, we found that CHI3L1 increased oxidative stress and fatty acid deposit, leading to abnormal accumulation of LPO. Furthermore, inhibition of LPO can substantially compromise the oncogenic effect of CHI3L1. Besides increased ROS and LPO, our in-vitro experiments also proved that CHI3L1 upregulates lipid oxidation enzymes including LOX and COX2. we also performed targeted oxylipin profiling, and identified activated AA metabolism by CHI3L1. The compounds of the AA cascade, such as prostaglandin E2 and leukotrienes, is known for their capability supporting cancer cell survival and proliferation [46]. Here we concluded that CHI3L1 promotes ROS synthesis and disturbs lipid homeostasis, thus accelerating HCC progression.

This study still has some limitations. Firstly, the research on the relationship between CHI3L1 level in muscle of cachetic model is simplistic. CHI3L1 is regarded as an important modulator in the process of inflammation and microenvironment remodeling. Besides liver, non-muscle organs including lymph node, spleen, adipose, and heart should also be taken into account. As well, we will construct muscle-specific Chi3l1 knockout mice to further identify the major origin of CHI3L1 in the circulation. Further validation in patient tissue is also demanded. Moreover, our study revealed the crosstalk between tumor and muscle mostly in cell lines. The subsequent validation such as organoids and therapy in mouse model would be performed in our future study.

In conclusion, sarcopenia is an independent risk factor for the outcomes in liver transplantation for HCC. Shown in the schematic diagram (Fig. 6J), CHI3L1 is up-regulated and secreted by the skeletal muscle to protect the muscle cells against inflammatory damage through TNF-α/TNF-R1 signaling. CHI3L1, in turn, potently disturbs lipid metabolism by promoting lipid peroxidation and fatty acid oxidation, and promotes HCC progression. In order to improve the outcomes of HCC patients, integrated therapy should also include novel strategies to ameliorate the sarcopenic condition.

Contributions

Study concept and design: XX and DL; Acquisition of data: ZL, ZC, HL, CH and WS; Analysis and interpretation of data: DL, RW, ZL, JZ, LX and MY; Drafting of the manuscript: DL, JZ, ZL, LP and WT; Critical revision of the manuscript for Important intellectual content: XX, SZ and XW; Statistical analysis: DL, ZL, JZ, LX and LP; Obtained funding: XX and DL; Administrative, technical, or material support: ZL, XY, HL and HC; Study supervision: XX. All authors have read and approved the article.

Declaration of competing interest

The authors declare that they have no known competing financial interests or personal relationships that could have appeared to influence the work reported in this paper.

Data availability

Data will be made available on request.

Appendix A. Supplementary data

Supplementary data to this article can be found online at https://doi.org/10.1016/j.redox.2022.102538.

References

[1] F. Bray, J. Ferlay, I. Soerjomataram, R.L. Siegel, L.A. Torre, A. Jemal, Global cancer statistics 2018: GLOBOCAN estimates of incidence and mortality worldwide for 36 cancers in 185 countries, CA A Cancer J. Clin. 68 (2018) 394–424, https://doi.org/10.3322/caac.21492.

[2] D.M. Parkin, F. Bray, J. Ferlay, P. Pisani, Global cancer statistics, 2002, CA A Cancer J. Clin. 55 (2005) 74–108, https://doi.org/10.3322/canjclin.55.2.74.

[3] E.G. Yegin, E. Oymaci, E. Karatay, A. Coker, Progress in surgical and nonsurgical approaches for hepatocellular carcinoma treatment, Hepatobiliary Pancreat. Dis. Int. 15 (2016) 234–256, https://doi.org/10.1016/s1499-3872(16)60097-8.

[4] E.Y. Kim, Y.S. Kim, J.Y. Seo, I. Park, H.K. Ahn, Y.M. Jeong, et al., The relationship between sarcopenia and systemic inflammatory response for cancer cachexia in small cell lung cancer, PLoS One 11 (2016), e0161125, https://doi.org/10.1371/journal.pone.0161125.

[5] G. Wang, A.K. Biswas, W. Ma, M. Kandpal, C. Coker, P.M. Grandgenett, et al., Metastatic cancers promote cachexia through ZIP14 upregulation in skeletal muscle, Nat. Med. 24 (2018) 770–781, https://doi.org/10.1038/s41591-018-0054-2.

[6] H.J. Patel, B.M. Patel, TNF-α and cancer cachexia: molecular insights and clinical implications, Life Sci. 170 (2017) 56–63, https://doi.org/10.1016/j.lfs.2016.11.033.

[7] S. Levolger, J.L. van Vugt, R.W. de Bruin, JN IJ. Systematic review of sarcopenia in patients operated on for gastrointestinal and hepatopancreatobiliary malignancies, Br. J. Surg. 102 (2015) 1448–1458, https://doi.org/10.1002/bjs.9893.

[8] T. Zhao, Z. Su, Y. Li, X. Zhang, Q. You, Chitinase-3 like-protein-1 function and its role in diseases, Signal Transduct. Targeted Ther. 5 (2020) 201, https://doi.org/10.1038/s41392-020-00303-7.

[9] D. Luo, H. Chen, P. Lu, X. Li, M. Long, X. Peng, et al., CHI3L1 overexpression is associated with metastasis and is an indicator of poor prognosis in papillary thyroid carcinoma, Cancer Biomarkers 18 (2017) 273–284, https://doi.org/10.3233/cbm-160255.

[10] S. Libreros, R. Garcia-Areas, P. Keating, N. Gazaniga, P. Robinson, A. Humbles, et al., Allergen induced pulmonary inflammation enhances mammary tumor growth and metastasis: role of CHI3L1, J. Leukoc. Biol. 97 (2015) 929–940, https://doi.org/10.1189/jlb.3A0214-114RR.

[11] P. Areshkov, S. Avdieiev, O. Balynska, D. Leroith, V. Kavsan, Two closely related human members of chitinase-like family, CHI3L1 and CHI3L2, activate ERK1/2 in 293 and U373 cells but have the different influence on cell proliferation, Int. J. Biol. Sci. 8 (2012) 39–48, https://doi.org/10.7150/ijbs.8.39.

[12] D.H. Lee, J.H. Han, Y.S. Lee, Y.S. Jung, Y.S. Roh, J.S. Yun, et al., Chitinase-3-like-1 deficiency attenuates ethanol-induced liver injury by inhibition of sterol regulatory element binding protein 1-dependent triglyceride synthesis, Metabolism 95 (2019) 46–56, https://doi.org/10.1016/j.metabol.2019.03.010.

[13] S. Zhang, A. Sousa, M. Lin, A. Iwano, R. Jain, B. Ma, et al., Role of chitinase 3-like 1 protein in the pathogenesis of hepatic insulin resistance in nonalcoholic fatty liver disease, Cells 10 (2021), https://doi.org/10.3390/cells10020201.

[14] H. Bartsch, J. Nair, Chronic inflammation and oxidative stress in the genesis and perpetuation of cancer: role of lipid peroxidation, DNA damage, and repair, Langenbeck's Arch. Surg. 391 (2006) 499–510, https://doi.org/10.1007/s00423-006-0073-1.

[15] U. Nair, H. Bartsch, J. Nair, Lipid peroxidation-induced DNA damage in cancer-prone inflammatory diseases: a review of published adduct types and levels in humans, Free Radic. Biol. Med. 43 (2007) 1109–1120, https://doi.org/10.1016/j.freeradbiomed.2007.07.012.

[16] S.M. Clemente, O.H. Martínez-Costa, M. Monsalve, A.K. Samhan-Arias, Targeting lipid peroxidation for cancer treatment, Molecules 25 (2020), https://doi.org/10.3390/molecules25215144.

[17] L.M. Teigen, A.J. Kuchnia, E. Nagel, C. Deuth, D.M. Vock, U. Mulasi, et al., Impact of software selection and ImageJ tutorial corrigendum on skeletal muscle measures at the third lumbar vertebra on computed tomography scans in clinical populations, JPEN - J. Parenter. Enter. Nutr. 42 (2018) 933–941, https://doi.org/10.1002/jpen.1036.

[18] A. Solomonica, [THE effect of air pollution on cardiovascular diseases], Harefuah 156 (2017) 586–588.

[19] E. Garreta-Lara, A. Checa, D. Fuchs, R. Tauler, S. Lacorte, C.E. Wheelock, et al., Effect of psychiatric drugs on Daphnia magna oxylipin profiles, Sci. Total Environ. 644 (2018) 1101–1109, https://doi.org/10.1016/j.scitotenv.2018.06.333.

[20] Q. Zhang, Y. Lou, J. Yang, J. Wang, J. Feng, Y. Zhao, et al., Integrated multiomic analysis reveals comprehensive tumour heterogeneity and novel immunophenotypic classification in hepatocellular carcinomas, Gut 68 (2019) 2019–2031, https://doi.org/10.1136/gutjnl-2019-318912.

[21] X. Xu, D. Lu, R. Zhuang, X. Wei, H. Xie, C. Wang, et al., The phospholipase A2 activity of peroxiredoxin 6 promotes cancer cell death induced by tumor necrosis factor alpha in hepatocellular carcinoma, Mol. Carcinog. 55 (2016) 1299–1308, https://doi.org/10.1002/mc.22371.

[22] J. Zhuo, D. Lu, Z. Lin, X. Yang, M. Yang, J. Wang, et al., The distinct responsiveness of cytokeratin 19-positive hepatocellular carcinoma to regorafenib, Cell Death Dis. 12 (2021) 1084, https://doi.org/10.1038/s41419-021-04320-4.

[23] Y.M. Naguib, A fluorometric method for measurement of peroxyl radical scavenging activities of lipophilic antioxidants, Anal. Biochem. 265 (1998) 290–298, https://doi.org/10.1006/abio.1998.2931.

[24] B. Sun, H. Luo, L. Deng, S. Zhang, Z. Chen, The study on mechanism of the modified Chinese herbal compound, jianpijiedu, on a mouse model of hepatic carcinoma cachexia, Mol. Med. Rep. 14 (2016) 3113–3121, https://doi.org/10.3892/mmr.2016.5602.

[25] N. Yabusaki, T. Fujii, S. Yamada, K. Suzuki, H. Sugimoto, M. Kanda, et al., Adverse impact of low skeletal muscle index on the prognosis of hepatocellular carcinoma after hepatic resection, Int. J. Surg. 30 (2016) 136–142, https://doi.org/10.1016/j.ijsu.2016.04.049.

[26] N. Harimoto, K. Shirabe, Y.I. Yamashita, T. Ikegami, T. Yoshizumi, Y. Soejima, et al., Sarcopenia as a predictor of prognosis in patients following hepatectomy for hepatocellular carcinoma, Br. J. Surg. 100 (2013) 1523–1530, https://doi.org/10.1002/bjs.9258.

[27] K.V. Chang, J.D. Chen, W.T. Wu, K.C. Huang, C.T. Hsu, D.S. Han, Association between loss of skeletal muscle mass and mortality and tumor recurrence in hepatocellular carcinoma: a systematic review and meta-analysis, Liver Cancer 7 (2018) 90–103, https://doi.org/10.1159/000484950.

[28] K. Fredriksson, I. Tjäder, P. Keller, N. Petrovic, B. Ahlman, C. Schéele, et al., Dysregulation of mitochondrial dynamics and the muscle transcriptome in ICU patients suffering from sepsis induced multiple organ failure, PLoS One 3 (2008), e3686, https://doi.org/10.1371/journal.pone.0003686.

[29] T.A. Zimmers, M.L. Fishel, A. Bonetto, STAT3 in the systemic inflammation of cancer cachexia, Semin. Cell Dev. Biol. 54 (2016) 28–41, https://doi.org/10.1016/j.semcdb.2016.02.009.

[30] Q.C. Qiu, L. Wang, S.S. Jin, G.F. Liu, J. Liu, L. Ma, et al., CHI3L1 promotes tumor progression by activating TGF-β signaling pathway in hepatocellular carcinoma, Sci. Rep. 8 (2018), 15029, https://doi.org/10.1038/s41598-018-33239-8.

[31] Y. Miyamoto, Y. Baba, Y. Sakamoto, M. Ohuchi, R. Tokunaga, J. Kurashige, et al., Sarcopenia is a negative prognostic factor After curative resection of colorectal cancer, Ann. Surg Oncol. 22 (2015) 2663–2668, https://doi.org/10.1245/s10434-014-4281-6.

[32] H. Fukushima, M. Yokoyama, Y. Nakanishi, K. Tobisu, F. Koga, Sarcopenia as a prognostic biomarker of advanced urothelial carcinoma, PLoS One 10 (2015), e0115895, https://doi.org/10.1371/journal.pone.0115895.

[33] N. Amini, G. Spolverato, R. Gupta, G.A. Margonis, Y. Kim, D. Wagner, et al., Impact total psoas volume on short- and long-term outcomes in patients undergoing curative resection for pancreatic adenocarcinoma: a new tool to assess sarcopenia, J. Gastrointest. Surg. 19 (2015) 1593–1602, https://doi.org/10.1007/s11605-015-2835-y.

[34] C.H. Wu, P.C. Liang, C.H. Hsu, F.T. Chang, Y.Y. Shao, T. Ting-Fang Shih, Total skeletal, psoas and rectus abdominis muscle mass as prognostic factors for patients with advanced hepatocellular carcinoma, J. Formos. Med. Assoc. 120 (2021) 559–566, https://doi.org/10.1016/j.jfma.2020.07.005.

[35] H. Uojima, H. Chuma, Y. Tanaka, H. Hidaka, T. Nakazawa, S. Iwabuchi, et al., Skeletal muscle mass influences tolerability and prognosis in hepatocellular carcinoma patients treated with lenvatinib, Liver Cancer 9 (2020) 193–206, https://doi.org/10.1159/000504604.

[36] G. Marasco, M. Serenari, M. Renzulli, L.V. Alemanni, B. Rossini, I. Pettinari, et al., Clinical impact of sarcopenia assessment in patients with hepatocellular carcinoma undergoing treatments, J. Gastroenterol. 55 (2020) 927–943, https://doi.org/10.1007/s00535-020-01711-w.

[37] T.C. Borges, T.L. Gomes, C. Pichard, A. Laviano, G.D. Pimentel, High neutrophil to lymphocytes ratio is associated with sarcopenia risk in hospitalized cancer patients, Clin. Nutr. 40 (2021) 202–206, https://doi.org/10.1016/j.clnu.2020.05.005.

[38] J.J. Pan, Y.S. Ge, G.L. Xu, W.D. Jia, W.F. Liu, J.S. Li, et al., The expression of chitinase 3-like 1: a novel prognostic predictor for hepatocellular carcinoma, J. Cancer Res. Clin. Oncol. 139 (2013) 1043–1054, https://doi.org/10.1007/s00432-013-1415-3.

[39] S.W. Görgens, K. Eckardt, M. Elsen, N. Tennagels, J. Eckel, Chitinase-3-like protein 1 protects skeletal muscle from TNFα-induced inflammation and insulin resistance, Biochem. J. 459 (2014) 479–488, https://doi.org/10.1042/bj20131151.

[40] A. Marquez-Quiñones, A. Cipak, K. Zarkovic, S. Fattel-Fazenda, S. Villa-Treviño, G. Waeg, et al., HNE-protein adducts formation in different pre-carcinogenic stages of hepatitis in LEC rats, Free Radic. Res. 44 (2010) 119–127, https://doi.org/10.3109/10715760903338071.

[41] K. Janion, E. Szczepańska, E. Nowakowska-Zajdel, K. Walkiewicz, J. Strzelczyk, Lipid peroxidation and total oxidant/antioxidant status in colorectal cancer patients, J. Biol. Regul. Homeost. Agents 34 (2020) 239–244, https://doi.org/10.23812/19-386-l.

[42] L. Lei, J. Yang, J. Zhang, G. Zhang, The lipid peroxidation product EKODE exacerbates colonic inflammation and colon tumorigenesis, Redox Biol. 42 (2021), 101880, https://doi.org/10.1016/j.redox.2021.101880.

[43] Y. Ni, C. Eng, Vitamin E protects against lipid peroxidation and rescues tumorigenic phenotypes in cowden/cowden-like patient-derived lymphoblast cells with germline SDHx variants, Clin. Cancer Res. 18 (2012) 4954–4961, https://doi.org/10.1158/1078-0432.Ccr-12-1055.

[44] G. Poli, G. Leonarduzzi, F. Biasi, E. Chiarpotto, Oxidative stress and cell signalling, Curr. Med. Chem. 11 (2004) 1163–1182, https://doi.org/10.2174/0929867043365323.

[45] Q. Gao, G. Zhang, Y. Zheng, Y. Yang, C. Chen, J. Xia, et al., SLC27A5 deficiency activates NRF2/TXNRD1 pathway by increased lipid peroxidation in HCC, Cell Death Differ. 27 (2020) 1086–1104, https://doi.org/10.1038/s41418-019-0399-1.

[46] T.I. Terpinskaya, A.V. Osipov, E.V. Kryukova, D.S. Kudryavtsev, N.V. Kopylova, T.L. Yanchanka, et al., α-Conotoxins and α-cobratoxin promote, while lipoxygenase and cyclooxygenase inhibitors suppress the proliferation of glioma C6 cells, Mar. Drugs 19 (2021), https://doi.org/10.3390/md19020118.